Distinct roles of the polarity factors Boi1 and Boi2 in the control of exocytosis and abscission in budding yeast

Aina Masgrau[a,b,†], Andrea Battola[a,b,†], Trinidad Sanmartin[a,b], Leszek P. Pryszcz[a,b], Toni Gabaldón[a,b,c], and Manuel Mendoza[a,b,‡,*]

[a]Centre for Genomic Regulation, The Barcelona Institute of Science and Technology, 08003 Barcelona, Spain; [b]Universitat Pompeu Fabra, 08003 Barcelona, Spain; [c]Institució Catalana de Recerca i Estudis Avançats, 08010 Barcelona, Spain

ABSTRACT **Boi1 and Boi2 (Boi1/2) are budding yeast plasma membrane proteins that function in polarized growth, and in cytokinesis inhibition in response to chromosome bridges via the NoCut abscission checkpoint. How Boi1/2 act in these two distinct processes is not understood. We demonstrate that Boi1/2 are required for a late step in the fusion of secretory vesicles with the plasma membrane of the growing bud. Cells lacking Boi1/2 accumulate secretory vesicles and are defective in bud growth. In contrast, Boi2 is specifically required for abscission inhibition in cells with chromatin bridges. The SH3 domain of Boi2, which is dispensable for bud growth and targets Boi2 to the site of abscission, is necessary and sufficient for abscission inhibition. Gain of function of the exocyst, a conserved protein complex involved in tethering of exocytic vesicles to the plasma membrane, rescued secretion and bud growth defects in *boi* mutant cells, and abrogated NoCut checkpoint function. Thus Boi2 functions redundantly with Boi1 to promote the fusion of secretory vesicles with the plasma membrane at sites of polarized growth, and acts as an abscission inhibitor during cytokinesis in response to chromatin bridges.**

Monitoring Editor
Patrick J. Brennwald
University of North Carolina

Received: Jun 19, 2017
Revised: Aug 31, 2017
Accepted: Sep 6, 2017

INTRODUCTION

Exocytosis, the delivery of secretory vesicles containing new membranes and membrane-remodeling factors to the plasma membrane (PM), is essential for cell growth and division. The molecular principles of exocytosis have been well characterized in the budding yeast *Saccharomyces cerevisiae*. In this organism, secretory vesicles are transported toward growth sites in the bud by actin-based transport; the actin cytoskeleton is in turn polarized by the localized activation of membrane-associated Cdc42 at the prospective bud site (Park and Bi, 2007). Secretory vesicles then fuse with the PM through soluble *N*-ethylmaleimide–sensitive factor attachment protein receptor (SNARE) complex formation. Prior to SNARE-mediated fusion with the target membrane, secretion requires a rate-limiting step known as "tethering," mediated by an evolutionarily conserved octameric complex, the exocyst (Wu *et al.*, 2008; He and Guo, 2009). Exocyst function is essential for cell growth and its inactivation leads to accumulation of exocytic vesicles in the cytoplasm (Novick *et al.*, 1980; Guo *et al.*, 1999; He *et al.*, 2007; Wu *et al.*, 2010). The Sec3 and Exo70 subunits associate directly with the PM in a manner that is largely independent of the actin cytoskeleton, whereas the other six subunits (Sec5, 6, 8, 10, 15, and 84) are transported to growth sites on membrane vesicles. This has led to the hypothesis that assembly of all subunits at the PM mediates vesicle tethering before fusion (Boyd *et al.*, 2004).

Exocytosis is also important for completion of cytokinesis. During this process, contraction of a membrane-associated actomyosin ring guides ingression of the PM at the site of cell division. Membrane resolution then splits the cell into two distinct topological units, in a process known as abscission (Green *et al.*, 2012;

This article was published online ahead of print in MBoC in Press (http://www.molbiolcell.org/cgi/doi/10.1091/mbc.E17-06-0404) on September 13, 2017.

†These authors contributed equally to this work.

The authors declare no conflicting financial interests.

‡Present address: Institute of Genetics and Molecular and Cellular Biology (IGBMC), 1 rue Laurent Fries, 67404 Illkirch, France.

*Address correspondence to: Manuel Mendoza (manuel.mendoza@igbmc.fr).

Abbreviations used: EM, electron microscopy; ESCRT, endosomal sorting complexes required for transport; GFP, green fluorescent protein; NAA, 1-naphthaleneacetic acid; PH, pleckstrin homology; PM, plasma membrane; PS, primary septum; SH3, SRC homology 3; SNARE, soluble *N*-ethymaleimide–sensitive factor attachment protein receptor; SNP, single nucleotide polymorphism; SPB, spindle pole body.

© 2017 Masgrau, Battola *et al.* This article is distributed by The American Society for Cell Biology under license from the author(s). Two months after publication it is available to the public under an Attribution–Noncommercial–Share Alike 3.0 Unported Creative Commons License (http://creativecommons.org/licenses/by-nc-sa/3.0).

"ASCB®," "The American Society for Cell Biology®," and "Molecular Biology of the Cell®" are registered trademarks of The American Society for Cell Biology.

Schiel and Prekeris, 2013). In HeLa cells, inactivation of the exocyst during cytokinesis leads to abscission defects (Gromley *et al.*, 2005). In budding yeast, actomyosin ring contraction at the site of division, called the bud neck, is coupled to synthesis of a chitin-based primary septum (PS). Yeast exocyst mutants show aberrant ring contraction dynamics, mislocalization of the PS chitin synthase Chs2, and cytokinesis defects suggesting that exocytosis is also required for late cell division steps in this organism (Dobbelaere and Barral, 2004; VerPlank and Li, 2005). The timing of abscission is monitored by a mechanism known as NoCut in budding yeast, and the abscission checkpoint in animal cells, which inhibits abscission in cells with chromatin bridges caught in the path of the cell division machinery (Steigemann *et al.*, 2009; Amaral *et al.*, 2016, 2017; Nähse *et al.*, 2016). Whether NoCut impinges on the exocytic machinery is not known.

The functionally redundant yeast cortical proteins Boi1 and Boi2 (Boi1/2) were previously implicated in polarized growth (Bender *et al.*, 1996; Matsui *et al.*, 1996) and in the NoCut abscission checkpoint (Norden *et al.*, 2006; Mendoza *et al.*, 2009). Boi1/2 associate with the bud cortex during bud growth and with the bud neck during cytokinesis, but how they act in these two distinct processes remained unclear. Here, we demonstrate that Boi1/2 promote vesicle exocytosis during bud growth. In contrast, the SH3 domain of Boi2, which targets the protein to the bud neck, is dispensable for bud growth but is specifically required to inhibit abscission in cells with chromatin bridges. Our results raise the possibility that Boi2 acts as both an activator of exocytosis and an inhibitor of abscission, depending on the cell cycle stage and the cellular response to chromosome segregation defects during cytokinesis.

RESULTS

Boi1 and Boi2 are essential for bud growth

Single *boi1*Δ and *boi2*Δ cells show normal growth and morphology but double deletion mutants display severe morphogenesis and growth defects (Supplemental Figure S1A; Bender *et al.*, 1996; Matsui *et al.*, 1996). To investigate the role of Boi1/2 during cell growth, we generated a conditional *boi1 boi2* null strain using an auxin-inducible degron (AID) to rapidly target Boi2 for polyubiquitination and proteasome-dependent degradation in the presence of 1-naphthaleneacetic acid (NAA) and the plant E2 ligase Tir1 (Figure 1A; Nishimura *et al.*, 2009). A *boi2-aid* strain expressing Tir1 grew well in complete media but failed to form colonies in the presence of NAA specifically in a *boi1*Δ background, consistent with an essential role of Boi1/2 in cell viability (Figure 1B).

To determine the consequences of Boi1/2 depletion on cell growth, wild-type and *boi1*Δ *boi2-aid* cells were examined by differential interference contrast (DIC) time-lapse microscopy 2 h after addition of 0.25 mM NAA, when Boi2-aid protein levels were reduced to nearly undetectable levels (Figure 1C). Wild-type and *boi1*Δ *boi2-aid* cells had similar morphology; however, Boi-depleted cells were severely impaired in surface growth. NAA-treated *boi1*Δ *boi2-aid* cells with small or medium buds grew at a slower rate or turned dark and stopped growing altogether (Figure 1D). Moreover, large round *boi1*Δ *boi2-aid* cells were observed 24 h after NAA addition (Figure 1E). Thus Boi1/2 function in cell growth, and depolarized growth previously reported in *boi1*Δ *boi2*Δ mutants (Bender *et al.*, 1996; Matsui *et al.*, 1996) might represent secondary defects associated with long-term Boi1/2 depletion.

Boi1/2 are dispensable for organization of actin and cell polarity factors

To assess whether Boi1/2 are required for maintenance of a polarized actin cytoskeleton, F-actin was visualized with fluorescently labeled phalloidin in wild-type and *boi1*Δ *boi2-aid* cells treated with NAA for 2 h. Actin patches and cables appeared similarly organized in wild-type and Boi-depleted cells (Figure 2A). In addition, we determined the localization of various cell polarity proteins fused to green fluorescent protein (GFP) in wild-type and Boi-depleted cells. Lack of Boi1/2 did not severely affect the localization of the Cdc42 guanine nucleotide exchange factor Cdc24, whereas it did moderately reduce that of the Boi-interacting protein Bem1 (McCusker *et al.*, 2007) and of the exocyst component Exo70 to the bud cortex. Furthermore, Boi-depleted cells showed slightly increased frequency of bud cortex localization of the Rab-like protein residing on post-Golgi vesicles, Sec4 (Figure 2B; Goud *et al.*, 1988). Thus Boi1/2 are not required for the maintenance of a polarized actin cytoskeleton and do not play a major role in the localization of polarity factors and exocytic vesicles to sites of polarized growth.

Identification of putative *boi1 boi2* suppressors by genome sequencing

To gain insight into the molecular functions of Boi1 and Boi2, we took advantage of a previously described *boi1*Δ *boi2*Δ strain, which was viable. These cells show no obvious morphological defects but are defective in the NoCut abscission checkpoint, which inhibits completion of cytokinesis in the presence of chromosome segregation defects (Norden *et al.*, 2006; Mendoza *et al.*, 2009). We hypothesized that this strain might contain one or more suppressor mutations (*SUP*) ensuring cell viability in the absence of Boi1/2. To identify putative suppressors, whole genome sequencing of this viable *boi1*Δ *boi2*Δ strain was performed and compared with its wild-type parent. Sequence analysis showed that gene order and copy number were identical between the two strains, ruling out aneuploidy and gross genome rearrangements in *boi1*Δ *boi2*Δ *SUP* (see *Materials and Methods* and Supplemental Figure S2). However, assessment of variation at the single nucleotide level identified 19 single nucleotide polymorphisms (SNPs) between *boi1*Δ *boi2*Δ *SUP* and its parental strain. Of these, seven were predicted to introduce amino acid changes in the encoded proteins (see Supplemental Table S1).

To determine linkage of SNPs to survival of *boi1*Δ *boi2*Δ *SUP* cells, genetic crosses were performed between this mutant and a *BOI1 BOI2* strain. As expected, a fraction of *boi1*Δ *boi2*Δ spores from this cross gave rise to viable colonies (Supplemental Figure S1B). One *boi1 boi2 SUP* clone was selected and backcrossed four more times; a *BOI1/boi1*Δ *BOI2/boi2*Δ *SUP/+* zygote that produced four viable spores was identified after the fifth backcross and its meiotic products were characterized by whole genome sequencing. Candidate suppressors should be present in both viable *boi1*Δ *boi2*Δ spores and absent in the two *BOI1 BOI2* clones; SNPs fulfilling these criteria are shown in Supplemental Table S2. Several SNPs clustered around specific genomic regions as expected by a selection sweep effect, presumably due to genetic background differences between *boi1*Δ *boi2*Δ *SUP* and the *BOI1 BOI2* strain (see *Materials and Methods*). However, the only SNP common to both the original and the backcrossed *boi1*Δ *boi2*Δ *SUP* segregants was located in the gene encoding the exocyst subunit Exo70, where it introduces one amino acid substitution (*EXO70-G388R*). Notably, the same mutation was independently isolated as a suppressor of *cdc42* and *rho3* mutants. The mutant protein, hereafter termed Exo70*, is expressed at a similar level to the wild-type protein and is incorporated into endogenous exocyst complexes, where it acts as a dominant, gain-of-function allele that suppresses the lethality and exocytosis defects of *cdc42* and *rho3* mutants (Wu *et al.*, 2010).

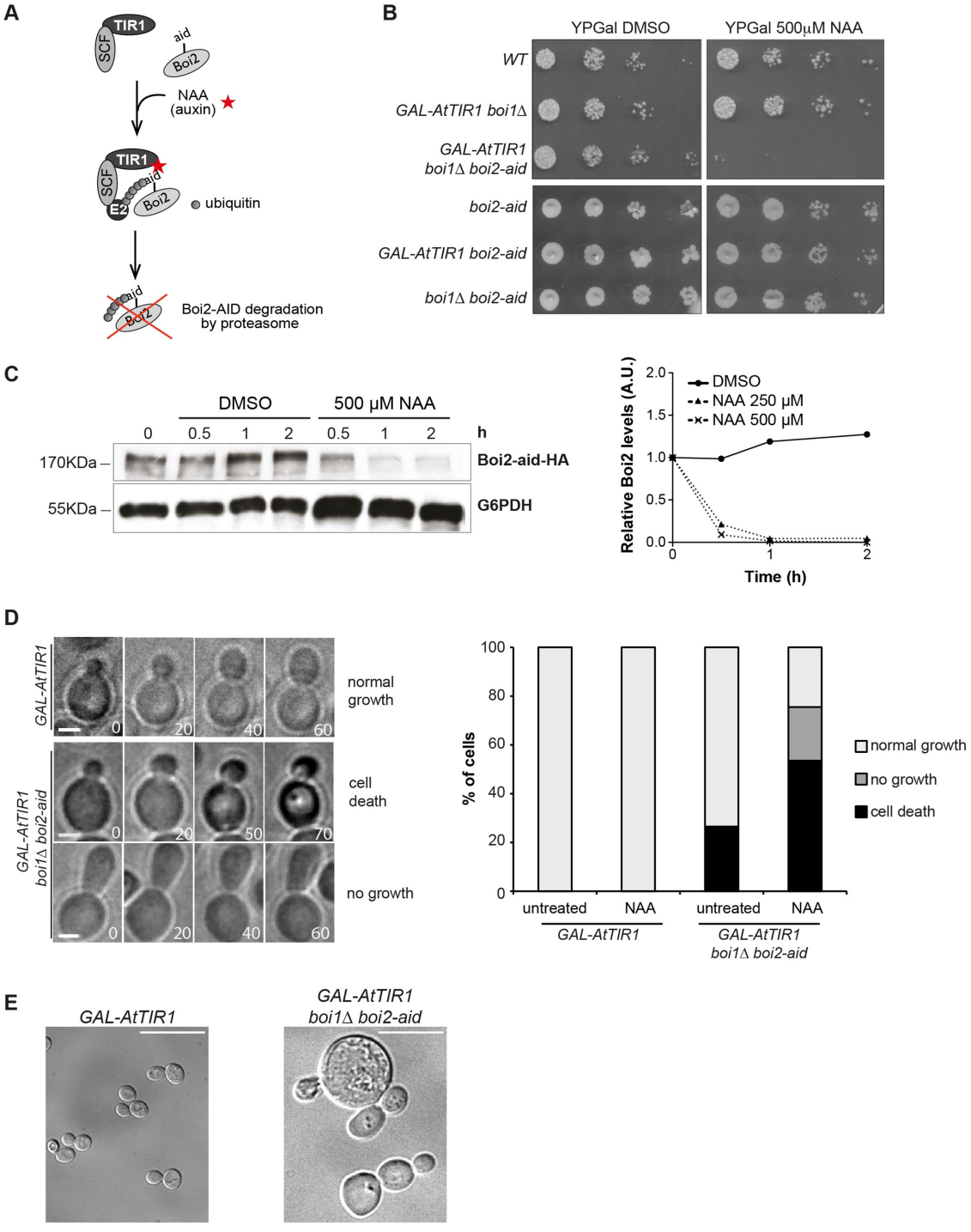

FIGURE 1: Boi1 and Boi2 are essential for bud growth. (A) Schematic representation of the auxin-induced degron system. SCF: Skp1, Cullin, and F-box complex. E2: E2 ubiquitin ligase. Aid: AID. (B) Serial dilutions of the indicated strains spotted onto the indicated plates and incubated for 3 d at 30°C. (C) *GAL-AtTIR1 boi1Δ boi2-aid-HA* cultures were grown in YPR to log phase, transferred to YPG for 2 h, and Boi2-aid-HA was detected by immunoblotting at the indicated time points after addition of dimethyl sulfoxide (DMSO) or the indicated concentrations of NAA. G6PDH was used as a loading control. (D) DIC time-lapse imaging of wild type and *boi1Δ boi2-aid* mutants expressing *GAL-AtTIR1*. Cells were grown in YPR to log phase, transferred to YPG for 2 h, and imaged in the presence of 250 μM NAA for the following 6 h. Cell images (4-μm-thick stacks spaced 0.8 μm) were acquired every 5 min; selected frames are shown. Time is represented in minutes. Scale bars, 2 μm. Cells were classified in three groups as indicated; the relative frequencies of these groups are indicated in the graph. $N > 23$ cells pooled from two independent experiments. (E) DIC images of wild-type and *boi1Δ boi2-aid* cells 24 h after addition of NAA. Scale bar, 10 μm.

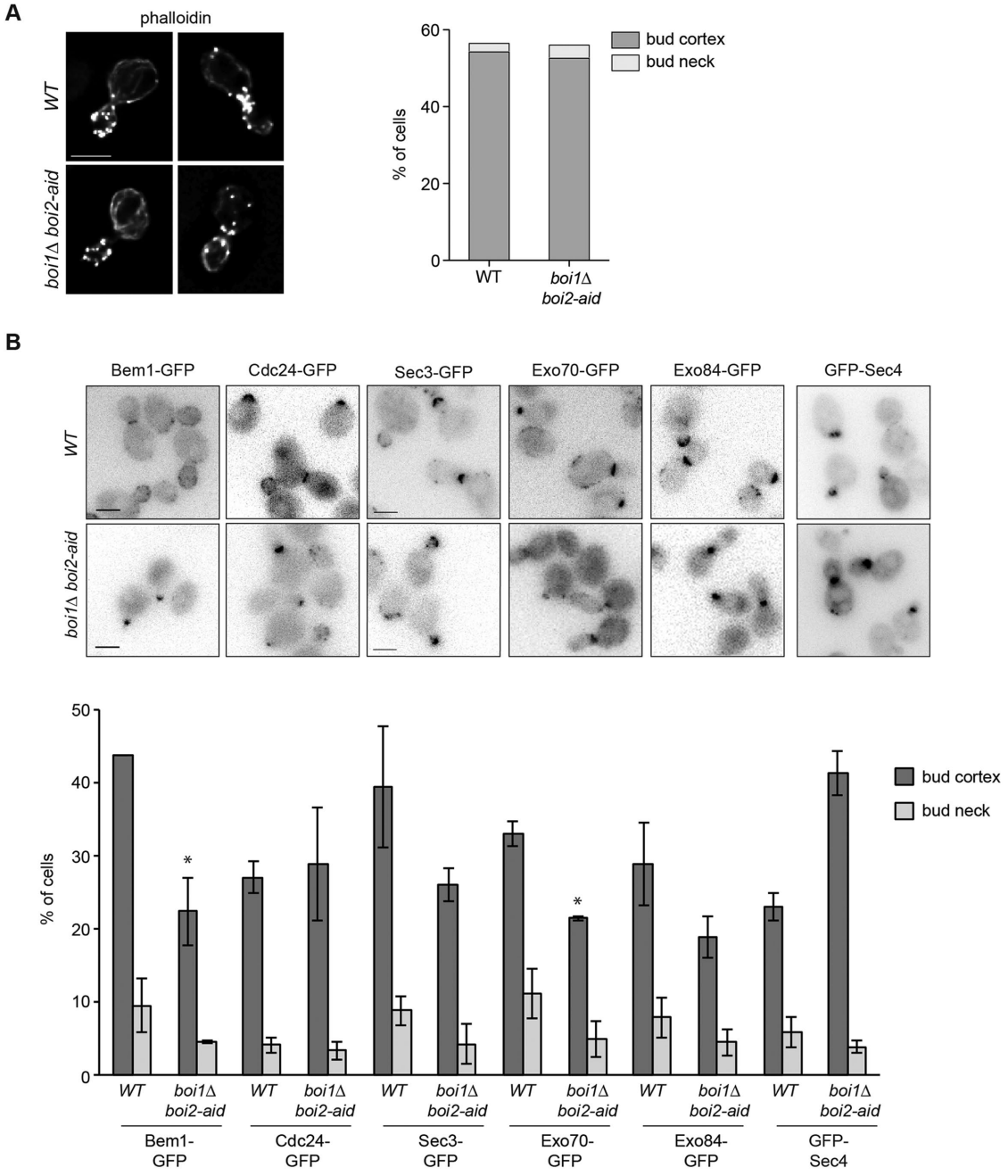

FIGURE 2: Boi1/2 are dispensable for actin organization or localization of cell polarity markers. (A) Distribution of filamentous actin (Alexa-488 phalloidin) in wild-type and *GAL-AtTIR1 boi1Δ boi2-aid* cells 2 h after NAA addition, treated as in Figure 1D ($N > 100$). Scale bars, 5 μm. (B) Localization of GFP fusion proteins in wild-type and *GAL-AtTIR1 boi1Δ boi2-aid* cells treated as in Figure 1D. All fusion proteins were expressed from their chromosomal locus except GFP-Sec4, which was expressed from a centromeric plasmid. Results are represented as mean and SEM ($N > 150$ cells for each condition, three to four independent experiments; *: $p < 0.05$, Student's *t* test).

Boi1/2 are required for vesicle exocytosis

To test whether *EXO70** is a dominant suppressor of the *boi1 boi2* mutant, centromeric plasmids encoding either the wild type or the dominant version of *EXO70* under the control of the regulatable *GAL1,10* promoter were introduced in *boi1Δ boi2-aid* strains. Galactose-driven expression of Exo70* was sufficient to restore the growth of Boi-deficient cells in the presence of NAA, whereas overexpression of wild-type Exo70 did not (Figure 3A). *EXO70** expressed from its natural promoter at the endogenous locus also supported the growth of both *boi1Δ boi2-aid* cells in NAA-containing media (Figure 3B) and of *boi* null strains, although *boi1Δ boi2Δ EXO70** strains grew at slower rates than wild type (Supplemental Figure S1C). Quantification of bud growth by DIC time-lapse microscopy showed that *boi1Δ boi2-aid EXO70** cells grew in a polarized manner and at slower rates than wild-type cells (Figure 3C). Together these results indicate that Boi1/2 promote exocyst-dependent vesicle fusion with the PM during bud growth.

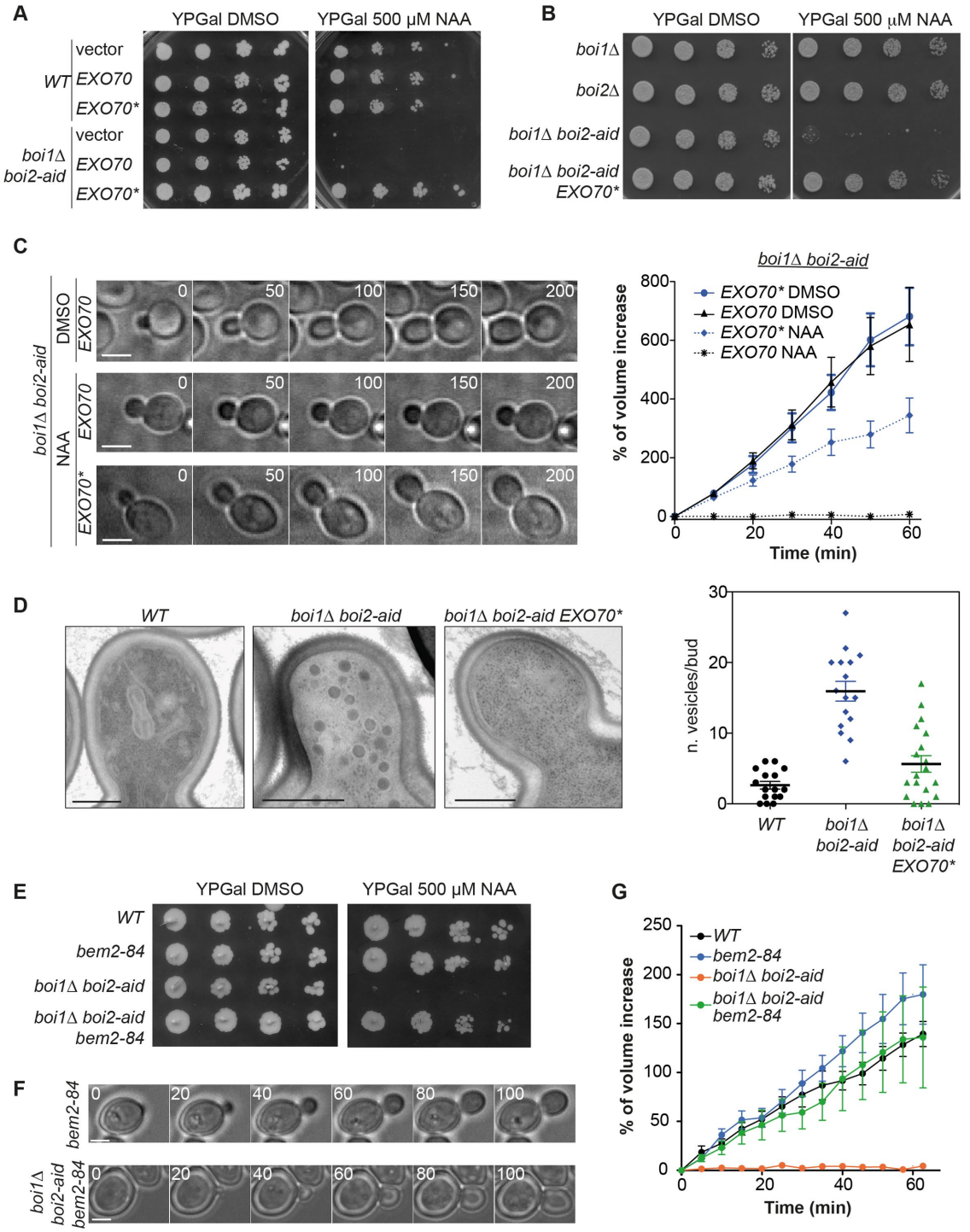

FIGURE 3: Boi1/2 are required for vesicle exocytosis. (A) Serial dilutions of wild-type or *boi1Δ boi2-aid* strains bearing *EXO70*, *EXO70**, or empty centromeric (*CEN*) plasmids were grown on galactose-containing media with and without NAA for 4 d. The plasmid-borne *EXO70* gene was under the control of the *GAL1* promoter. (B) Serial dilutions of cells of the indicated strains grown on YPG with and without NAA for 3 d. *EXO70** is expressed from the *EXO70* promoter at the endogenous locus. (C) DIC time-lapse images of *boi1Δ boi2-aid* cells transformed with *EXO70* or *EXO70* CEN* plasmids. Cells were grown in SC Gal-Leu to log phase, and imaged 2 h after the addition of 250 µM NAA at 25°C. Numbers indicate time in minutes; scale bar, 5 µm. The graph represents the relative increase in volume of individual buds over time. $N = 10$ cells per condition. Error bars indicate SEM. (D) EM images of small budded cells in the indicated mutants. Cells were treated as in Figure 1C and fixed 2 h after NAA addition; scale bar, 500 nm. The number of vesicles/cell/section is represented in the graph ($N > 15$). Lines represent the mean; bars are SEM. (E) Serial dilutions of the indicated strains grown for 4 d at 30°C. (F) DIC time-lapse images of cells treated as in C, but imaged at 27°C. Time is indicated in minutes; scale bar, 2 µm. (G) Relative increase in bud volume over time for cells of the indicated strains as in C. $N = 19$ (*WT*), 13 (*bem2-84*), 14 (*boi1Δ boi2-aid*), 10 (*bem2-84 boi1Δ boi2-aid*).

To directly assess this, electron microscopy (EM) analysis was performed in wild-type and Boi-depleted cells. In wild-type cells few secretory vesicles are detected by EM due to high basal secretion rates. In contrast, a higher number of 80–100-nm-diameter vesicles were visualized in NAA-treated *boi1Δ boi2-aid* cells (Figure 3D). Secretory vesicles were particularly abundant near the surface of small and medium-sized buds, in a manner reminiscent of exocyst loss-of-function mutants. Conversely, vesicle accumulation was largely alleviated *in boi1Δ boi2-aid EXO70** cells (Figure 3D). Thus Boi1 and Boi2 may promote the tethering function of the exocyst to allow secretory vesicles to fuse with the PM.

Cdc42 and Rho3 GTPases are thought to directly activate the exocyst through their interaction with Exo70 (Wu *et al.*, 2010). As viability of *boi1 boi2* cells is rescued by overexpression of Rho3 or its functionally related GTPase Rho4 (Bender *et al.*, 1996; Matsui *et al.*, 1996) and by expression of *EXO70** (this study), Boi proteins might act together with Rho GTPases in exocyst activation. Deletion of the GTPase-activating proteins (GAP) *RGA1* or *RGA2* (targeting Cdc42) or *RGD1* (acting on Rho3 and Rho4) (Stevenson *et al.*, 1995; Roumanie *et al.*, 2000; Smith *et al.*, 2002) did not restore the growth of *boi1Δ boi2-aid* strains in NAA (Supplemental Figure S3). In contrast, the GAP-deficient *bem2-84* mutation, which leads to Cdc42 hyperactivation (Atkins *et al.*, 2013) allowed Boi-depleted cells to survive and restored their normal growth, suggesting a specific role for Bem2 in the control of exocytosis through hyperactivation of Rho-GTPase signaling (Figure 3, E–G). Thus Boi1/2 might promote activation of the exocyst together with multiple Rho-like GTPases regulated by Bem2, such as Cdc42 and potentially Rho4 (Gong *et al.*, 2013) during bud growth.

Boi1/2 are required for secretion of specific exocytic vesicles

We then tested whether Boi1 and Boi2 are required for the secretion of specific protein cargoes. Budding yeast cells have two major types of exocytic vesicles, which can be distinguished by their density and protein content: light vesicles containing cell wall–remodeling cargo like the endoglucanase Bgl2, and dense vesicles typified by the presence of invertase (Harsay and Bretscher, 1995). The activity of secreted periplasmic invertase in wild-type and Boi-depleted cells was determined using a standard assay (Goldstein and Lampen, 1975). Exocyst mutant cells (*sec6-4*) known to be impaired in secretion of invertase showed a strong reduction in the activity of the secreted form of this enzyme at the restrictive temperature, relative to wild-type cells (Figure 4A; He *et al.*, 2007). In contrast, *boi1Δ boi2-aid* cells showed no reduction of secreted invertase activity after incubation with NAA to deplete Boi2, suggesting that Boi1/2 are not required for secretion of invertase-containing vesicles (Figure 4A). To assay secretion of Bgl2, immunoblots were used to probe the internal fraction of the enzyme in spheroplasts of wild-type and mutant cells. Both *sec14-1* cells previously reported to be blocked in secretion of Bgl2 at 37°C (Curwin *et al.*, 2009), and Boi-depleted cells accumulated large amounts of Bgl2 in the cytoplasm relative to the total cellular content. This defect was fully reversed in the *boi1Δ boi2-aid EXO70** strain (Figure 4B and Supplemental Figure S4). Thus Boi1/2 function is dispensable for secretion of invertase vesicles but is essential for exocytosis of Bgl2-type vesicles, and this requirement can be bypassed by gain of function of the exocyst.

Interestingly, the localization of Boi2 to sites of membrane remodeling was dependent on the exocyst, as Boi2-GFP was rapidly lost from the cell cortex and bud neck in *sec6* and *sec8* temperature-sensitive (ts) mutants shifted to the restrictive temperature (Figure 5).

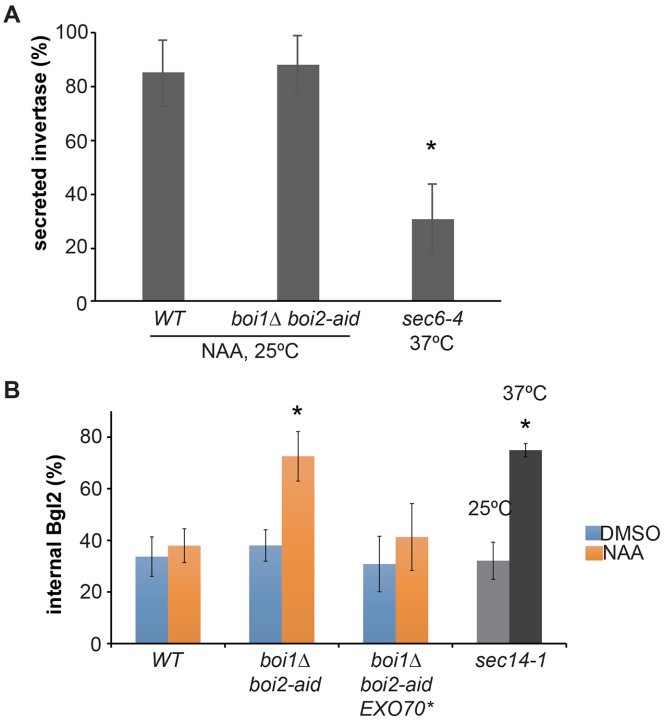

FIGURE 4: Boi1/2 are essential for secretion of Bgl2 but not invertase. (A) Activity of secreted invertase in wild-type and *boi1Δ boi2-aid* cells treated with NAA for 2 h, and of *sec6-4* cells shifted to 37°C for 2 h. Invertase secretion is the ratio of external invertase activity relative to total (internal + external) activity. Invertase data are the mean and SEM of five independent experiments performed in triplicate. (B) Internal Bgl2 levels of cells of the indicated strains after incubation with DMSO or NAA for 2 h (*boi1Δ boi2-aid*), or after shift to 37°C for 2 h (*sec14-1*). Bgl2 levels were determined by Western blot and represent the ratio between internal and total (internal + external). G6PDH was used as a loading control. Bgl2 data are the mean and SD of three independent experiments. *: $p < 0.05$, Student's *t* test.

This opens the possibility that Boi proteins are recruited to exocytic sites by the exocyst complex, either directly or indirectly, to regulate sorting of specific vesicles for exocyst-dependent secretion.

Boi2 inhibits cytokinesis in cells with catenated chromatin bridges

We next addressed the role of Boi1/2 in cytokinesis. Anaphase chromatin bridges lead to inhibition of abscission; this inhibition was bypassed in *boi1Δ boi2Δ* cells, leading to the conclusion that Boi1/2 function at the bud neck as abscission inhibitors (Norden *et al.*, 2006; Mendoza *et al.*, 2009). Our finding that Boi-deficient cells used in these studies contained the *EXO70** suppressor is in line with their lack of growth defects, but raised the possibility that their failure to inhibit abscission could be partially or even completely due to exocyst gain of function, and not to loss of Boi1/2. To address these issues, we revisited the role of Boi1/2 in cytokinesis. Wild-type, *boi1Δ* and *boi2Δ* cells were released from a G1 arrest and shifted to 37°C to induce chromatin bridges by inactivation of topoisomerase II with the *top2-4* mutation (Holm *et al.*, 1985). The spindle pole body (SPB) marker Spc42-GFP was used to monitor progression through mitosis, whereas contraction and subsequent resolution of the PM at the bud neck were monitored using GFP fused to the PM targeting CAAX motif of Ras2 (Amaral *et al.*, 2016).

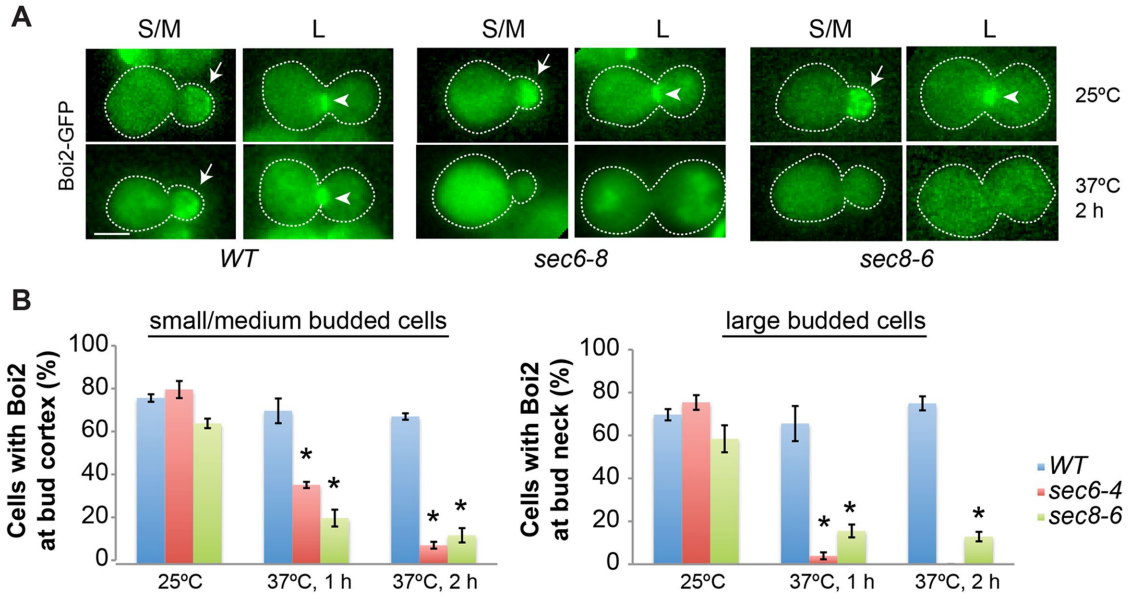

FIGURE 5: Boi2 localization depends on exocyst function. (A) Boi2-GFP localization in representative wild-type and exocyst mutant cells. Wild-type, *sec6-4* and *sec8-6* strains were grown at 25°C to mid log phase and shifted to 37°C for the indicated times. Boi2-GFP localization at the bud cortex (arrows) was scored in cells with small and medium buds (S/M), whereas localization at the bud neck (arrowheads) was scored in cells with large buds (L); scale bar, 5 μm. (B) Quantification of Boi2-GFP localization for cells shown in (A) for the indicated strains and categories. Mean and SD are shown ($N = 3$ experiments, >70 cells per experiment). *: $p < 0.05$, Student's *t* test.

Live fluorescence microscopy showed that wild-type cells underwent ingression of the PM at the bud neck after entry of the SPB in the bud, and this was followed by membrane resolution into two distinct layers as previously reported (abscission) (Figure 6, A and B). In *boi1*Δ and *boi2*Δ cells, ingressed bud neck membranes resolved with dynamics similar to those of wild-type cells (Figure 6, A and B). In contrast, *top2-4* and *top2-4 boi1*Δ mutants showed ingression of the PM at the bud neck but were impaired or severely delayed in its resolution, consistent with a defect in abscission in *top2* mutants (Figure 6, A and C) as previously observed by fluorescence microscopy and EM tomography (Amaral *et al.*, 2016). However, analysis of GFP-CAAX showed that unlike *top2-4* and *top2-4 boi1*Δ mutants, most *top2-4 boi2*Δ cells were able to complete abscission (Figure 6, A and C). Therefore Boi2 is specifically required for inhibition of abscission in cells with catenated chromatin bridges, whereas Boi1 is dispensable for this inhibition.

The SH3 domain of Boi2 is necessary and sufficient for inhibition of cytokinesis

Boi1 and Boi2 share a similar domain organization, featuring a Pleckstrin-homology (PH) domain at their C-terminus and a Src-homology 3 (SH3) domain at their N-terminus. Boi1/2 PH domains can interact with PM lipids and associate with the bud cortex; moreover, the PH domain of Boi1 is required for viability of *boi1 boi2* mutant cells (Hallett *et al.*, 2002; Yu *et al.*, 2004). Therefore PH domains mediate the essential function of Boi1/2 in bud growth. In contrast, the SH3 domain of Boi1 is not required for viability of *boi* null mutants and targets Boi1 to the bud neck (Hallett *et al.*, 2002). We therefore asked whether the SH3 domain of Boi2 might be required for its bud neck localization and its function in abscission inhibition. A version of Boi2 expressed under the control of the weak GalS promoter, and lacking the 102 N-terminal amino acids spanning the SH3 domain, did not perturb Boi2 targeting to the bud cortex, but abrogated its localization to the bud neck during cytokinesis (Figure 7A). This Boi2 mutant version (Boi2Δ^{SH3}) also supported normal bud growth and abscission in *boi1*Δ cells (Figure 7B). However, *boi1*Δ *GalS-boi2*Δ^{SH3} cells did not inhibit abscission in the presence of chromatin bridges caused by topoisomerase-II inactivation (Figure 7B). Furthermore, a C-terminal truncation of Boi2 at position 103, which removed most of the protein but retained only the SH3 domain (SH3$_{Boi2}$) was recruited to the bud cortex and bud neck (Figure 7C) and supported abscission inhibition in cells with chromatin bridges (Figure 7D). Thus the SH3 domain of Boi2 is not essential for bud growth, but is specifically required for Boi2 targeting to the bud neck and is sufficient for its function in the NoCut abscission checkpoint.

Exocyst gain of function restores abscission in cells with chromatin bridges

As inhibition of the exocyst perturbs the completion of yeast cytokinesis (Dobbelaere and Barral, 2004; VerPlank and Li, 2005), we asked whether gain of function of the exocyst can prevent its inhibition. To this end, the GFP-CAAX reporter was used to monitor abscission in *EXO70** cells with normal and defective chromosome segregation. *EXO70** cells completed abscission with similar kinetics to those of wild type, and importantly, failed to inhibit abscission in the presence of catenated DNA bridges (Figure 8A). These results raise the possibility that abscission inhibition in cells with chromatin bridges requires modulation of exocyst-dependent, membrane-remodeling events at the abscission site. To gain insight into cytokinesis membrane trafficking events in cells with chromatin bridges, we followed the kinetics of the vesicle marker Sec4, which accumulates in the bud neck at the end of mitosis and controls membrane trafficking during cytokinesis (Figure 8B; Lepore *et al.*, 2016). The levels of Sec4-GFP accumulating in the bud neck relative to total Sec4 cellular levels were significantly

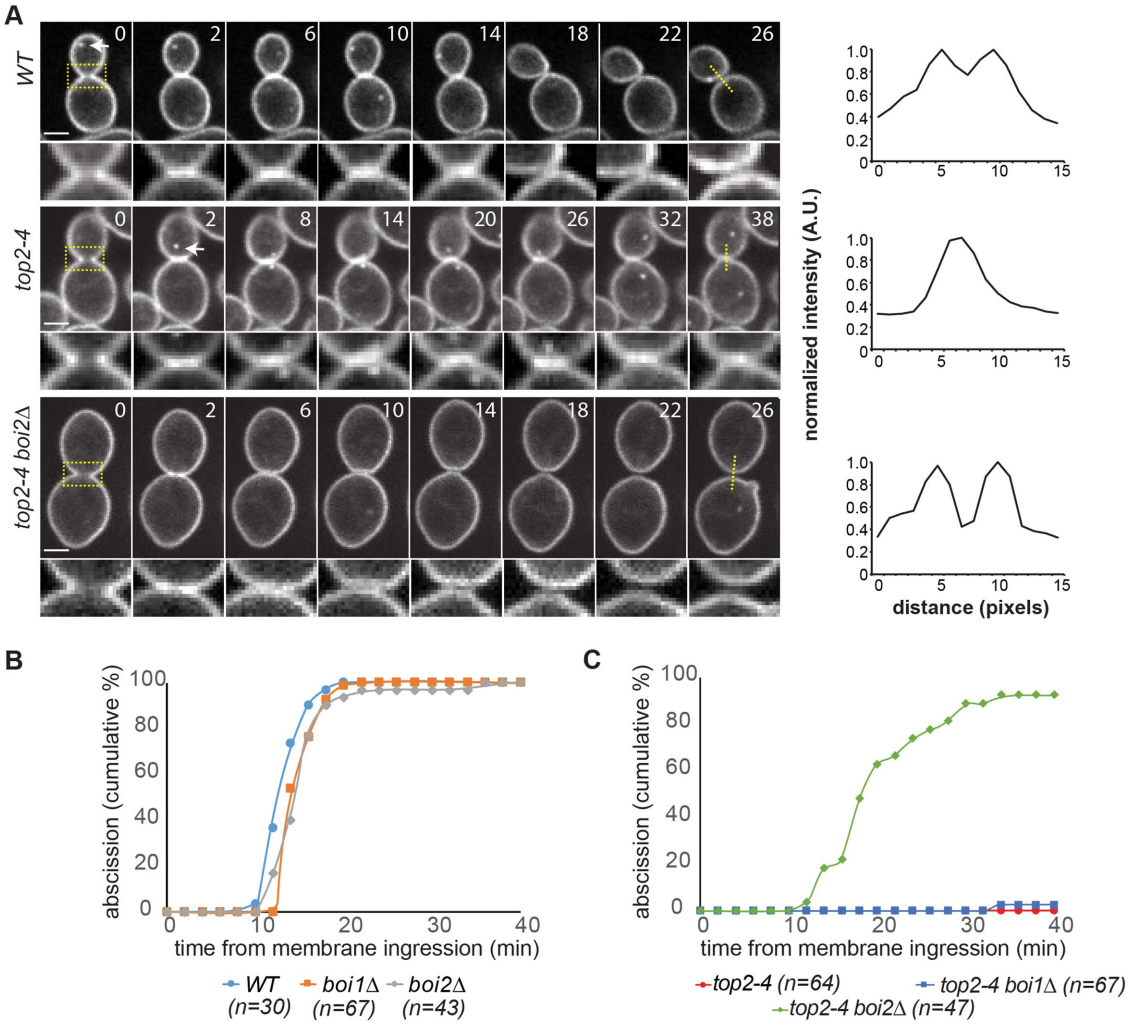

FIGURE 6: Boi2 is required for inhibition of abscission in topoisomerase-II deficient cells. (A) Membrane ingression and abscission in representative cells of the indicated strains. *Z*-stacks spaced 0.3 µm apart and spanning the whole cell were acquired at 2-min intervals, but only central *Z*-planes are shown. Whole-cell images are shown at the top and enlargements of the bud neck region at the bottom. The spindle pole marker Spc42–GFP (visible only in some *Z*-sections; arrows) allowed the simultaneous visualization of spindle elongation. Numbers indicate time in minutes; time 0 marks the frame before membrane ingression. To analyze the status of the bud neck membrane, the GFP fluorescence intensity was measured across the cleavage plane in the central *Z*-plane (yellow lines) shown in the right. A reduction in local intensity marked membrane resolution and was scored as abscission (top and bottom graphs); a single peak denoted the preabscission stage (middle). (B, C) Graphs show the fraction of cells completing abscission relative to the time of membrane ingression. Cells were synchronized in G1 with α-factor in YPD at 25°C and shifted to 37°C 15 min before release from the G1 block. Data are from cells pooled from two to four independent experiments.

higher in *top2-4* cells than in wild-type cells. Moreover, increased Sec4 levels at the bud neck in the presence of chromatin bridges were restored in *EXO70** cells but not in *boi2*Δ cells (Figure 8, B and C, and Supplemental Figure S5). Thus cytokinetic membrane remodeling is altered in response to DNA decatenation defects, in a process that can be bypassed by gain of function of the exocyst.

DISCUSSION

Role of Boi1/2 in vesicle exocytosis during polarized growth

In this study, we demonstrate that Boi1/2 are essential for exocytosis of specific vesicle types, and for bud growth. We find that inhibition of exocytosis caused by Boi1/2 depletion is rescued by gain of function of the exocyst and by hyperactivation of GTPase signaling (in *EXO70** and *bem2-ts* mutants, respectively). Because the exocyst subunit Exo70 is an effector of the GTPases Cdc42 and Rho3 (Wu *et al.*, 2010), our results raise the possibility that Boi1/2 act by GTPase-mediated up-regulation of the exocyst. Boi1/2 could achieve this by facilitating the proper assembly of exocyst-activating complexes. Supporting this model, Boi1 and Boi2 interact with multiple proteins involved in polarized growth including the Cdc42 exchange factor Cdc24 and Bem1 (McCusker *et al.*, 2007), which in turn associates with exocyst complex (Liu and Novick, 2014). Moreover, Boi1/2 interact with exocyst components in vitro and by two-hybrid assays (Tonikian *et al.*, 2009) and we find that recruitment of Boi2 to sites of membrane remodeling depends on exocyst function. Boi1/2-dependent up-regulation of the exocyst could then promote vesicle

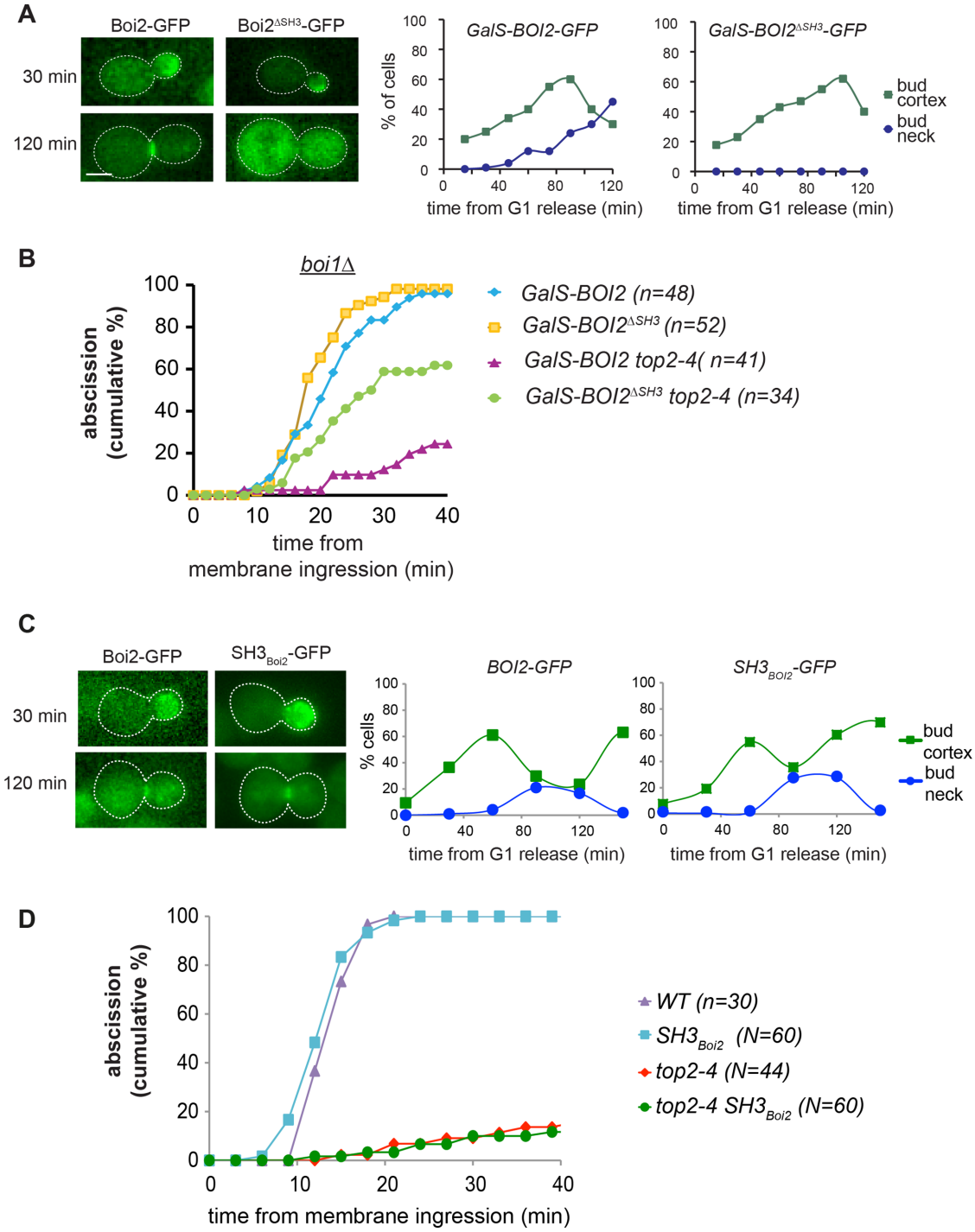

FIGURE 7: The SH3 domain of Boi2 is necessary and sufficient for abscission inhibition. (A) Cells of the indicated strains were released from a G1 block and imaged at time intervals in galactose-containing media. The localization of Boi2 to either the cortex or the bud neck (left) was determined by wide-field microscopy ($N > 30$ cells/time point). (B) Abscission analysis as in Figure 6, except that the cultures were grown to mid log phase in galactose-containing media. Data are from cells pooled from two to three independent experiments. (C) Localization of Boi2-GFP and $SH3_{Boi2}$-GFP as in A, except that cells were released from a G1 block and imaged in glucose-containing media ($N > 70$ cells/time point). (D) Abscission analysis as in B except that cells were grown in glucose-containing media. Data are from cells pooled from three independent experiments.

fusion with the PM by SNARE complexes. Accordingly, a recent study reported that both the exocyst and the SNARE-associated protein Sec1 interact with Boi1/2, and that overexpression of Sec1 restores exocytosis in Boi-depleted cells (Kustermann *et al.*, 2017).

Our results suggest that Boi1/2 function in secretion of Bgl2-containing vesicles, but not of invertase vesicles. Most exocyst mutants (including *exo70* alleles) are blocked in secretion of both vesicle types (Novick *et al.*, 1980; Harsay and Bretscher, 1995; Guo *et al.*, 1999; Wu *et al.*, 2010). However, the hypomorphic *exo70-35* and

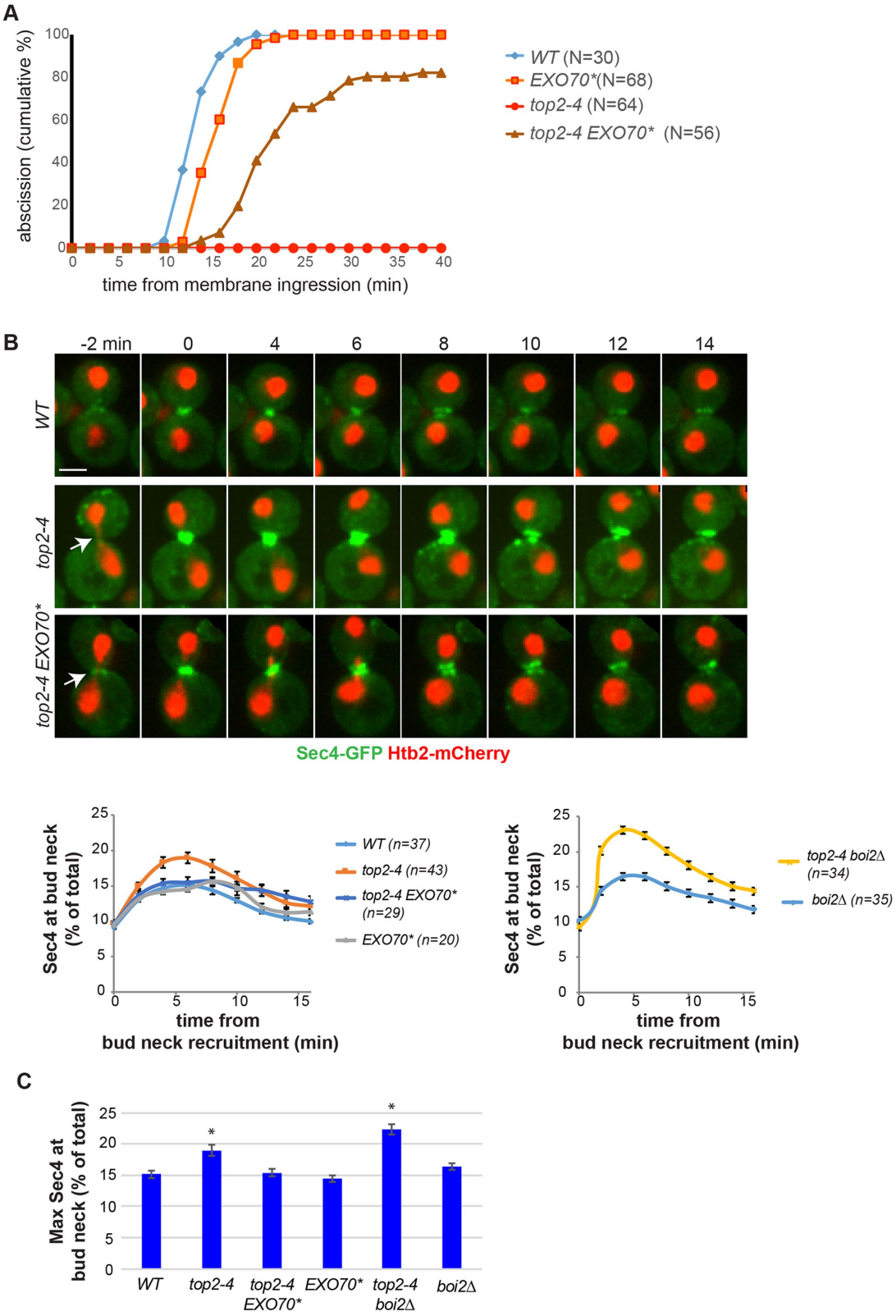

FIGURE 8: *EXO70** is a suppressor of abscission defects in topoisomerase-II-deficient cells. (A) Abscission analysis as in Figure 5, A and B. Data are from cells pooled from two to three independent experiments. (B) Localization of Sec4-GFP and histone 2B (Htb2) fused to mCherry in late mitotic cells. Arrows mark chromatin bridges in *top2-4* mutants. Time 0 marks the appearance of Sec4 at the bud neck. Levels of Sec4-GFP at the bud neck, expressed as percent of the total GFP fluorescence in the cell, were measured in sum projections of confocal *Z*-stacks spanning the entire cell. Mean and SEM are shown. Data are from cells pooled from two to four experiments. (C) Maximal levels (mean and SEM) of Sec4-GFP at the bud neck of the indicated strains. Asterisks denote statistically significant differences from the wild type ($p < 0.05$, Student's *t* test).

exo70-38 mutants, like Boi1/2-depleted cells, are specifically impaired in secretion of Bgl2 but not invertase vesicles (He *et al.*, 2007). Therefore Boi1/2 might specifically target Bgl2 (and perhaps other) vesicles for tethering by exocyst complexes during bud growth.

Role of Boi2 in inhibition of abscission

In both yeast and human cells, chromatin bridges can cause inhibition of abscission through the NoCut abscission checkpoint, but the molecular mechanisms involved remain poorly understood. In human cells, this process involves regulation of the endosomal sorting complex required for transport (ESCRT) III complex, which associates with the PM at the site of cytokinesis and regulates abscission timing (Carlton *et al.*, 2012). Our data indicates that in yeast, abscission inhibition relies on association of the SH3 domain of Boi2 with the abscission site. Although both Boi-dependent functions, in polarized growth and abscission, may involve PM-remodeling processes, the relevant molecular mechanisms could be distinct. Indeed, the essential role of Boi1 and Boi2 for polarized growth and exocytosis depends on their PH domains, which are required for association with the bud cortex and are essential for cell viability (Hallett *et al.*, 2002; Kustermann *et al.*, 2017). In contrast, we find that the SH3 domain of Boi2 is dispensable for viability, but is both necessary and sufficient for bud neck targeting and inhibition of abscission. Interestingly, the SH3 domains of Boi1 and Boi2 can interact with exocyst components (Tonikian *et al.*, 2009), and the exocyst is required for Boi2 recruitment to the bud neck. Whether direct Boi2-exocyst interactions are relevant for the control of abscission in cells with chromosome segregation defects remains an important question for future studies.

It has been suggested that Rho-like GTPases mediate exocyst activation through the induction of conformational changes in Exo70 (Wu *et al.*, 2008). This allosteric regulation model was further supported by the identification of point mutations in *EXO70*, including *EXO70**, that support growth of *cdc42* and *rho3* mutants defective in exocytosis (Wu *et al.*, 2010). Our finding that *EXO70** mutants are defective in the NoCut checkpoint suggests that allosteric regulation of the exocyst may play a key role in the regulation of abscission timing in yeast, and perhaps also in human cells. Exo70* complexes might be refractory to modulation by Boi1/2, thereby enabling multiple exocytic pathways independently of Boi1/2 or topoisomerase-II defects, and explaining proper growth of *boi1 boi2 EXO70** and normal cytokinesis in *top2-ts EXO70** mutants. Accumulation of Sec4-GFP at the abscission site in *top2-ts* cells may thus represent inhibition of exocytosis during cytokinesis. Consistent with this idea, inhibition of the exocyst prevents completion of abscission in budding yeast (Dobbelaere and Barral, 2004). EM imaging failed to detect vesicles in the vicinity of the bud neck during cytokinesis in *top2* mutants (Amaral *et al.*, 2016, and unpublished data), but this could be due to the short time during which Sec4 accumulates at the bud neck during cytokinesis. Alternatively, accumulation of Sec4 in the bud neck of *top2* mutant cells may reflect alterations in a nonexocytic membrane-remodeling process such as endocytosis, which can also be regulated by the exocyst (Jose *et al.*, 2015). A detailed characterization of specific membrane and protein trafficking events during abscission, and the potential role of exocyst complexes in regulating these processes, should provide valuable insight into the mechanisms of abscission regulation in response to chromatin bridges.

MATERIALS AND METHODS

Strains and media

S. cerevisiae strains are derivatives of S288c, except *boi1Δ boi2Δ* and its parental wild-type strain (kind gifts from E. Bailly, INSERM) which have the BFA264-15D background. Yeast cells were grown in YPD/YPG/YPR (1% bacto-yeast extract; 2% bacto-peptone; 2% dextrose, galactose or raffinose; and 0.004% adenine). Gene tagging and deletions were generated by standard PCR-based methods. The *EXO70** (G488R) plasmid was generated by site-directed mutagenesis (Quickchange; Stratagene) of a *GAL1-EXO70* centromeric vector (Open Biosystems). To integrate *EXO70** in its native locus in S288c strains, *EXO70** was tagged with the HA-natNT2 cassette (Janke *et al.*, 2004) in *boi1Δ boi2Δ SUP*, and a PCR-derived fragment of *EXO70*-HA:natNT2* was used in a one-step allele replacement; correct strains were identified by sequencing. PB3065 (*bem2-84 LEU2/Bgl*II) (Atkins *et al.*, 2013) was used for one-step gene replacement at the *BEM2* locus, and the mutation was confirmed by sequencing.

Time-lapse and fluorescence microscopy

Time-lapse microscopy was performed on cells in log phase, or after synchronization with α-factor as indicated, plated in minimal synthetic medium in concanavalin A-coated Lab-Tek chambers (Nunc) and placed in a preequilibrated temperature-controlled chamber. Imaging was performed using a Cell Observer HS microscope with a 100×, 1.4 NA objective and an AxioCam MrX camera (Zeiss) (Figures 1 and 3), an AF6000 wide-field microscope (Leica) with a 100×, 1.4 NA objective and an iXon 885 DU EM-CCD camera (Andor Technology; Figures 2 and 5C), or a Revolution XD spinning disk confocal microscope with a 100×, 1.45 NA objective and an iXon 897E Dual Mode EM-CCD camera (Andor Technology; Figures 5 and 6 and Supplemental Figure S4). Bud volumes were calculated from DIC stacks using ImageJ and the BudJ plug-in (Ferrezuelo *et al.*, 2012) customized for analysis of *Z*-stacks. To visualize F-actin, cells were fixed with 3.7% formaldehyde for 1 h, washed in phosphate-buffered saline (PBS), incubated with 0.2 U/ml Alexa 488-phalloidin for 1 h at 25°C, washed in PBS and visualized immediately in 80% glycerol/20% PBS. Abscission assays were performed as in Amaral *et al.* (2016). Briefly, the PM was visualized via *GAL1-10* promoter driven GFP-CAAX integrated in the *HIS3* locus. Expression of GFP-CAAX in glucose media was driven by the chimeric *ADH1pr*-Gal4-ER-VP16 transcription factor (Louvion *et al.*, 1993) (*URA3*; gift from Francesc Posas, Universitat Pompeu Fabra) and addition of 90 nM β-estradiol (Sigma) 2 h before imaging. Only cells starting cytokinesis (membrane ingression) at least 40 min before the end of image acquisition were considered for the quantifications of abscission. Fluorescence intensities were measured from single sections of each cell to score membrane separation (abscission).

Electron microscopy

Cells were cryoimmobilized using an EM HPM 100 high-pressure freezer (Leica), freeze-substituted in anhydrous acetone containing 2% glutaraldehyde and 0.1% uranyl acetate (Figure 3) or 2% OsO_4 and 0.1% uranyl acetate (Figure 5) and warmed to room temperature (EM AFS-2; Leica). After several acetone rinses, cells were incubated with 1% tannic acid, washed, incubated with OsO_4 at 1% acetone, washed again, infiltrated with Epon resin and embedded and polymerized at 60°C. Ultrathin sections were obtained using an Ultracut UC6 ultramicrotome (Leica) and observed in a Tecnai Spirit electron microscope (FEI, The Netherlands) equipped with a Megaview III CCD camera.

Sequencing and bioinformatics analysis

Strains were sequenced using Illumina Genome Analyzer II or HiSeq paired-end technology. Reads were trimmed before the genome assembly at the base with quality lower than 20 using FASTX-Toolkit (Cold Spring Harbor Laboratory; http://hannonlab.cshl.edu/fastx_toolkit). Subsequently reads shorter than 31 bases (and their

pairs) were discarded. Assemblies for each strain were created de novo using Velvet v. 1.1.02 (Zerbino and Birney, 2008). The insert size of the paired-end reads was estimated by aligning reads onto the assembly created from single reads. The optimal k-mer length (*k*) for each strain was chosen using VelvetOptmiser.pl to maximize the total number of bases in contigs longer than 1 kb (Lbp). In addition, we used autoestimation of coverage cutoff and removed contigs shorter than 1 kb. Supplemental Table S3 lists detailed information about each resulting assembly. Genomic reads were aligned onto the Saccharomyces Genome Database (SGD) reference strain using Bowtie2 v. 2.0.0-beta7 (Langmead and Salzberg, 2012). SNPs were detected using bam2snp.ref.py v1.0. In brief, SNPs were called at sites with different genotypes in a given strain than in the wild-type strain. Only SNPs with high coverage (≥10×) and low ambiguity (≥90% of aligned reads call the same nucleotide at that position) at both the mapped reads of the given mutant strain and the reference were accepted. This filtering procedure was able to discard likely false-positive SNPs.

Depth-of-coverage variation was analyzed with IGV v 2.3.32 (Thorvaldsdóttir *et al.*, 2013) to identify potential duplications or deletions. In addition, we analyzed read pairs with incongruent distance or orientation to identify possible rearrangements, that is, inversions, deletions, duplications, or translocations using bam2sv.py v1.0b. Finally, we used de novo contigs aligned against wild-type reference assembly as an independent line of evidence for potential rearrangements detection. Alignments were created by MUMer v3.07 with default parameters (Kurtz *et al.*, 2004). Only best reciprocal matches were further accepted, but partial overlaps between matches were allowed. A minimal alignment length of 65 base pairs was set as a threshold. In addition, cutoff of 200 base pairs was set for deletion detection.

Genomic libraries were deposited to Short Read Archive (PRJEB7711). bam2sv.py and bam2snp.ref.py are available at https://bitbucket.org/lpryszcz/bin.

Secretion assays

Invertase secretion was assessed essentially as described previously (Goldstein and Lampen, 1975). Briefly, cells were grown to logarithmic phase and transferred to 0.1% glucose YPDA to induce invertase expression, either in the presence of 90 nM β-estradiol and 0.5 mM NAA (to respectively induce Gal1-*At*Tir1 and Boi2 degradation in *boi1*Δ *boi2-aid*) or at 37°C (for *sec6-4*). After 2 h, cells were centrifuged and washed with cold 10 mM NaN_3, and equal cell numbers were transferred to tubes with 10 mM NaN_3/0.2% Triton X-100, which were then vortexed and freeze-thawed (total invertase pool), and 10 mM NaN_3 (external pool). In triplicate, adjusted amounts of sample were diluted in 0.1 M sodium acetate (pH 5.1) and 0.5 M sucrose was added at timed intervals to measure invertase activity. Reactions were stopped after 30 min with 0.2 M KPO_4, pH 7/10 mM *N*-ethylmaleimide, and boiled. Glucose was detected with GO Assay Kit (Sigma) according to manufacturer's instructions.

Bgl2 accumulation was determined as described (Curwin *et al.*, 2012) with minor modifications. Cells were grown in YPR to log phase, transferred to YPG for 2 h, and cells were either shifted to 37°C (*sec14-1*) or incubated with 0.5 mM NAA (*boi1*Δ *boi2-aid*). After 2 h, equal cell numbers were harvested by centrifugation and washed in 10 mM NaN_3/NaF solution. Total protein extracts were prepared by trichloroacetic acid extraction. For the internal fraction, cells were resuspended in prespheroplasting buffer (100 mM Tris-H_2SO_4, pH 9.4; 50 mM β-mercaptoethanol; 10 mM NaN_3; 10 mM NaF) and washed with spheroplasting buffer without zymolyase (50 mM KH_2PO_4-KOH, pH 7.4; 1.4 M sorbitol; 10 mM NaN_3). Then cells were resuspended in spheroplasting buffer containing 167 µg/ml zymolyase 100T (Seikagaku Biobusiness) and incubated with gentle mixing. Spheroplasts were harvested and resuspended in sample buffer before separation by SDS–PAGE and Western blotting to detect Bgl2 (specific antibody gift from Randy Schekman, University of California, Berkeley) and glucose-6-phosphate dehydrogenase (G6PDH) as a loading control (Sigma).

ACKNOWLEDGMENTS

We are grateful to Karolina Jodkowska for assistance with the initial characterization of *EXO70**. We thank Yves Barral, Amy Curwin, Vivek Malhotra, Snezhana Oliferenko, Isabelle Sagot, Jerome Solon, and members of the Mendoza laboratory for helpful suggestions; Marti Aldea, Eric Bailly, Derek McCusker, David Pellman, and Randy Schekman for providing reagents; the CRG Genomics and Advanced Light Microscopy Units; and the CCiT Electron Cryomicroscopy Unit (Universitat de Barcelona). This research is supported by grants from the Spanish Ministry of Economy and Competitiveness (BFU09-08213 and BFU2012-37162 to M.M. and BIO2012-37161 to T.G.), the Qatar National Research Fund (NPRP 5-298-3-086 to T.G.), and the European Research Council (ERC Starting Grant 260965 to M.M. and 310325 to T.G.). L.P.P. was funded through La Caixa–CRG International Fellowship Program.

REFERENCES

Amaral N, Brownlow N, Mendoza M (2017). DNA replication stress: NoCut to the rescue. Cell Cycle 16, 233–234.

Amaral N, Vendrell A, Funaya C, Idrissi F-Z, Maier M, Kumar A, Neurohr G, Colomina N, Torres-Rosell J, Geli M-A, Mendoza M (2016). The Aurora-B-dependent NoCut checkpoint prevents damage of anaphase bridges after DNA replication stress. Nat Cell Biol 18, 516–526.

Atkins BD, Yoshida S, Saito K, Wu CF, Lew DJ, Pellman D (2013). Inhibition of Cdc42 during mitotic exit is required for cytokinesis. J Cell Biol 202, 231–240.

Bender L, Lo HS, Lee H, Kokojan V, Peterson V, Bender A (1996). Associations among PH and SH3 domain-containing proteins and Rho-type GTPases in yeast. J Cell Biol 133, 879–894.

Boyd C, Hughes T, Pypaert M, Novick P (2004). Vesicles carry most exocyst subunits to exocytic sites marked by the remaining two subunits, Sec3p and Exo70p. J Cell Biol 167, 889–901.

Carlton JG, Caballe A, Agromayor M, Kloc M, Martin-Serrano J (2012). ESCRT-III governs the Aurora B-mediated abscission checkpoint through CHMP4C. Science 336, 220–225.

Curwin AJ, Fairn GD, McMaster CR (2009). Phospholipid transfer protein Sec14 is required for trafficking from endosomes and regulates distinct trans-Golgi export pathways. J Biol Chem 284, 7364–7375.

Curwin AJ, von Blume J, Malhotra V (2012). Cofilin-mediated sorting and export of specific cargo from the Golgi apparatus in yeast. Mol Biol Cell 23, 2327–2338.

Dobbelaere J, Barral Y (2004). Spatial coordination of cytokinetic events by compartmentalization of the cell cortex. Science 305, 393–396.

Ferrezuelo F, Colomina N, Palmisano A, Garí E, Gallego C, Csikasz-Nagy A, Aldea M (2012). The critical size is set at a single-cell level by growth rate to attain homeostasis and adaptation. Nat Commun 3, 1012.

Goldstein A, Lampen JO (1975). Beta-D-fructofuranoside fructohydrolase from yeast. Methods Enzymol 42, 504–511.

Gong T, Liao Y, He F, Yang Y, Yang DD, Chen XD, Gao XD (2013). Control of polarized growth by the Rho family GTPase Rho4 in budding yeast: requirement of the N-terminal extension of Rho4 and regulation by the Rho GTPase-activating protein Bem2. Eukaryot Cell 12, 368–377.

Goud B, Salminen A, Walworth NC, Novick PJ (1988). A GTP-binding protein required for secretion rapidly associates with secretory vesicles and the plasma membrane in yeast. Cell 53, 753–768.

Green RA, Paluch E, Oegema K (2012). Cytokinesis in animal cells. Annu Rev Cell Dev Biol 28, 29–58.

Gromley A, Yeaman C, Rosa J, Redick S, Chen C-T, Mirabelle S, Guha M, Sillibourne J, Doxsey SJ (2005). Centriolin anchoring of exocyst and SNARE complexes at the midbody is required for secretory-vesicle-mediated abscission. Cell 123, 75–87.

Guo W, Grant A, Novick P (1999). Exo84p is an exocyst protein essential for secretion. J Biol Chem 274, 23558–23564.

Hallett MA, Lo HS, Bender A (2002). Probing the importance and potential roles of the binding of the PH-domain protein Boi1 to acidic phospholipids. BMC Cell Biol 3, 16.

Harsay E, Bretscher A (1995). Parallel secretory pathways to the cell surface in yeast. J Cell Biol 131, 297–310.

He B, Guo W (2009). The exocyst complex in polarized exocytosis. Curr Opin Cell Biol 21, 537–542.

He B, Xi F, Zhang J, TerBush D, Zhang X, Guo W (2007). Exo70p mediates the secretion of specific exocytic vesicles at early stages of the cell cycle for polarized cell growth. J Cell Biol 176, 771–777.

Holm C, Goto T, Wang JC, Botstein D (1985). DNA topoisomerase II is required at the time of mitosis in yeast. Cell 41, 553–563.

Janke C, Magiera MM, Rathfelder N, Taxis C, Reber S, Maekawa H, Moreno-Borchart A, Doenges G, Schwob E, Schiebel E, Knop M (2004). A versatile toolbox for PCR-based tagging of yeast genes: new fluorescent proteins, more markers and promoter substitution cassettes. Yeast 21, 947–962.

Jose M, Tollis S, Nair D, Mitteau R, Velours C, Massoni-Laporte A, Royou A, Sibarita J-B, McCusker D (2015). A quantitative imaging-based screen reveals the exocyst as a network hub connecting endocytosis and exocytosis. Mol Biol Cell 26, 2519–2534.

Kurtz S, Phillippy A, Delcher AL, Smoot M, Shumway M, Antonescu C, Salzberg SL (2004). Versatile and open software for comparing large genomes. Genome Biol 5, R12.

Kustermann J, Wu Y, Rieger L, Dedden D, Phan T, Walther P, Dünkler A, Johnsson N (2017). The cell polarity proteins Boi1p and Boi2p stimulate vesicle fusion at the plasma membrane of yeast cells. J Cell Sci 130, 2996–3008.

Langmead B, Salzberg SL (2012). Fast gapped-read alignment with Bowtie 2. Nat Methods 9, 357–359.

Lepore D, Spassibojko O, Pinto G, Collins RN (2016). Cell cycle-dependent phosphorylation of Sec4p controls membrane deposition during cytokinesis. Science 214, 691–703.

Liu D, Novick P (2014). Bem1p contributes to secretory pathway polarization through a direct interaction with Exo70p. J Cell Biol 207, 59–72.

Louvion JF, Havaux-Copf B, Picard D (1993). Fusion of GAL4-VP16 to a steroid-binding domain provides a tool for gratuitous induction of galactose-responsive genes in yeast. Gene 131, 129–134.

Matsui Y, Matsui R, Akada R, Toh-e A (1996). Yeast src homology region 3 domain-binding proteins involved in bud formation. J Cell Biol 133, 865–878.

McCusker D, Denison C, Anderson S, Egelhofer TA, Yates JR, Gygi SP, Kellogg DR (2007). Cdk1 coordinates cell-surface growth with the cell cycle. Nat Cell Biol 9, 506–515.

Mendoza M, Norden C, Durrer K, Rauter H, Uhlmann F, Barral Y (2009). A mechanism for chromosome segregation sensing by the NoCut checkpoint. Nat Cell Biol 11, 477–483.

Nähse V, Christ L, Stenmark H, Campsteijn C (2016). The abscission checkpoint: making it to the final cut. Trends Cell Biol 27, 1–11.

Nishimura K, Fukagawa T, Takisawa H, Kakimoto T, Kanemaki M (2009). An auxin-based degron system for the rapid depletion of proteins in nonplant cells. Nat Methods 6, 917–922.

Norden C, Mendoza M, Dobbelaere J, Kotwaliwale CV, Biggins S, Barral Y (2006). The NoCut pathway links completion of cytokinesis to spindle midzone function to prevent chromosome breakage. Cell 125, 85–98.

Novick P, Field C, Schekman R (1980). Identification of 23 complementation groups required for post-translational events in the yeast secretory pathway. Cell 21, 205–215.

Park HO, Bi E (2007). Central roles of small GTPases in the development of cell polarity in yeast and beyond. Microbiol Mol Biol Rev 71, 48–96.

Roumanie O, Peypouquet MF, Bonneu M, Thoraval D, Doignon F, Crouzet M (2000). Evidence for the genetic interaction between the actin-binding protein Vrp1 and the RhoGAP Rgd1 mediated through Rho3p and Rho4p in *Saccharomyces cerevisiae*. Mol Microbiol 36, 1403–1414.

Schiel JA, Prekeris R (2013). Membrane dynamics during cytokinesis. Curr Opin Cell Biol 25, 92–98.

Smith GR, Givan SA, Cullen P, Sprague GF (2002). GTPase-activating proteins for Cdc42. Eukaryot Cell 1, 469–480.

Steigemann P, Wurzenberger C, Schmitz MHA, Held M, Guizetti J, Maar S, Gerlich DW (2009). Aurora B-mediated abscission checkpoint protects against tetraploidization. Cell 136, 473–484.

Stevenson BJ, Ferguson B, De Virgilio C Bi E, Pringle JR, Ammerer G, Sprague GF (1995). Mutation of RGA1, which encodes a putative GTPase-activating protein for the polarity-establishment protein Cdc42p, activates the pheromone-response pathway in the yeast *Saccharomyces cerevisiae*. Genes Dev 9, 2949–2963.

Thorvaldsdóttir H, Robinson JT, Mesirov JP (2013). Integrative Genomics Viewer (IGV): high-performance genomics data visualization and exploration. Briefings Bioinf 14, 178–192.

Tonikian R, Xin X, Toret CP, Gfeller D, Landgraf C, Panni S, Paoluzi S, Castagnoli L, Currell B, Seshagiri S, *et al*. (2009). Bayesian modeling of the yeast SH3 domain interactome predicts spatiotemporal dynamics of endocytosis proteins. PLoS Biol 7, e1000218.

VerPlank L, Li R (2005). Cell cycle-regulated trafficking of Chs2 controls actomyosin ring stability during cytokinesis. Mol Biol Cell 16, 2529–2543.

Wu H, Rossi G, Brennwald P (2008). The ghost in the machine: small GTPases as spatial regulators of exocytosis. Trends Cell Biol 18, 397–404.

Wu H, Turner C, Gardner J, Temple B, Brennwald P (2010). The Exo70 subunit of the exocyst is an effector for both Cdc42 and Rho3 function in polarized exocytosis. Mol Biol Cell 21, 430–442.

Yu JW, Mendrola JM, Audhya A, Singh S, Keleti D, DeWald DB, Murray D, Emr SD, Lemmon MA (2004). Genome-wide analysis of membrane targeting by *S. cerevisiae* pleckstrin homology domains. Mol Cell 13, 677–688.

Zerbino DR, Birney E (2008). Velvet: algorithms for de novo short read assembly using de Bruijn graphs. Genome Res 18, 821–829.